GPR56-related bilateral frontoparietal polymicrogyria: further evidence for an overlap with the cobblestone complex

Nadia Bahi-Buisson,[1,2,3,4,*] Karine Poirier,[2,3,*] Nathalie Boddaert,[5,6] Catherine Fallet-Bianco,[7,8] Nicola Specchio,[9] Enrico Bertini,[10] Okay Caglayan,[11] Karine Lascelles,[12] Caroline Elie,[13] Jérôme Rambaud,[1,2,3] Michel Baulac,[14] Isabelle An,[14] Patricia Dias,[15] Vincent des Portes,[16] Marie Laure Moutard,[17] Christine Soufflet,[18] Monique El Maleh,[19] Cherif Beldjord,[20] Laurent Villard[21,22] and Jamel Chelly[2,3]

1 Service de Neurologie pédiatrique, Assistance Publique-Hôpitaux de Paris (AP-HP), hôpital Necker, Paris, France
2 Institut Cochin, Université Paris-Descartes, CNRS (UMR 8104), Paris, France
3 Inserm, U1016, Paris, France
4 Inserm, U663, Paris, F-75015 France; University Paris Descartes, Faculty of Medicine, Paris, F-75005 France
5 Service de Radiologie Pédiatrique, AP-HP, hôpital Necker, Paris, France
6 Inserm, U797- INSERM-CEA, Service Hospitalier Frédéric Joliot, CEA, 4, place du General Leclerc, 91406, Orsay, France
7 Department of Neuropathology, Sainte-Anne Hospital, Paris-Descartes, France
8 University, INSERM U894 'Glial Plasticity' Paris, 75014, France
9 Division of Neurology, Department of Neurosciences, Ospedale Bambino Gesu', Rome, Italy
10 Unit of Molecular Medicine, Department of Neurosciences, Ospedale Bambino Gesu', Rome, Italy
11 Kayseri Education and Research Hospital Head, Department of Medical Genetics, 38010, Kayseri, Turkey
12 Evelina Children's Hospital, London, UK
13 Biostatistics Hopital Necker Enfants Malades, Université Paris Descartes, APHP, 149 rue de Sevres 75015 Paris France
14 Service de Neurologie, AP-HP, Hopital Pitie-Salpetriere, Paris, France Universite Paris VI, France
15 Medical Genetics Department, Santa Maria's Hospital, Lisbon, Portugal
16 Service de Neurologie pédiatrique, HFME, Bron, HCL, Université Lyon1, France
17 Service de Neurologie Pediatrique, AP-HP, Hopital Trousseau, Paris, France
18 Unité d'Electrophysiologie AP-HP, Hôpital Necker, Paris, France
19 Service de Radiologie Pédiatrique, AP-HP, hôpital Robert Debre, Paris, France
20 Service de Biologie Moleculaire et Genetique, Pavillon Cassini AP-HP, Hôpital Cochin, Paris, France
21 Inserm, U910, Faculté de Médecine, Marseille, F-13000, France
22 Aix-Marseille Université, Faculté de Médecine, F-13000, France

*These authors contributed equally to this work.

Correspondence to: Nadia Bahi-Buisson, MD, PhD,
Paediatric Neurology Hopital Necker Enfants Malades,
Université Paris Descartes,
APHP,149 rue de Sèvres,
75015 Paris, France
E-mail: nadia.bahi-buisson@nck.aphp.fr

***GPR56* mutations cause an autosomal recessive polymicrogyria syndrome that has distinctive radiological features combining bilateral frontoparietal polymicrogyria, white matter abnormalities and cerebellar hypoplasia. Recent investigations of a *GPR56* knockout mouse model suggest that bilateral bifrontoparietal polymicrogyria shares some features of the cobblestone brain malformation and demonstrate that loss of *GPR56* leads to a dysregulation of the maintenance of the pial basement membrane**

integrity in the forebrain and the rostral cerebellum. In light of these findings and other data in the literature, this study aimed to refine the clinical features with the first description of a foetopathological case and to define the range of cobblestone-like features in *GPR56* bilateral bifrontoparietal polymicrogyria in a sample of 14 patients. We identified homozygous *GPR56* mutations in 14 patients from eight consanguineous families with typical bilateral bifrontoparietal polymicrogyria and in one foetal case, out of 30 patients with bifrontoparietal polymicrogyria referred for molecular screening. The foetal case, which was terminated at 35 weeks of gestation in view of suspicion of Walker Warburg syndrome, showed a cobblestone-like lissencephaly with a succession of normal, polymicrogyric and 'cobblestone-like' cortex with ectopic neuronal overmigration, agenesis of the cerebellar vermis and hypoplastic cerebellar hemispheres with additional neuronal overmigration in the pons and the cerebellar cortex. The 14 patients with *GPR56* mutations (median 8.25 years, range 1.5–33 years) were phenotypically homogeneous with a distinctive clinical course characterized by pseudomyopathic behaviour at onset that subsequently evolved into severe mental and motor retardation. Generalized seizures (12/14) occurred later with onset ranging from 2.5 to 10 years with consistent electroencephalogram findings of predominantly anterior bursts of low amplitude α-like activity. Neuroimaging demonstrated a common phenotype with bilateral frontoparietally predominant polymicrogyria (13/13), cerebellar dysplasia with cysts mainly affecting the superior vermis (11/13) and patchy to diffuse myelination abnormalities (13/13). Additionally, the white matter abnormalities showed a peculiar evolution from severe hypomyelination at 4 months to patchy lesions later in childhood. Taken as a whole, these observations collectively demonstrate that *GPR56* bilateral bifrontoparietal polymicrogyria combines all the features of a cobblestone-like lissencephaly and also suggest that *GRP56*-related defects produce a phenotypic continuum ranging from bilateral bifrontoparietal polymicrogyria to cobblestone-like lissencephaly.

Keywords: polymicrogyria; neuronal migration disorders; cobblestone lissencephaly; *GPR56*; pial basement membrane; radial glia cells

Abbreviation: BFPP = bilateral bifrontoparietal polymicrogyria

Introduction

Bilateral bifrontoparietal polymicrogyria [BFPP; OMIM® (http://www.ncbi.nlm.nih.gov/omim) 606854] is in most cases a recessively inherited genetic disorder of human cerebral cortical development, characterized by abnormal cortical lamination and gyral organization that is more severe in the frontal and parietal lobes (Piao *et al.*, 2002; Chang *et al.*, 2003). BFPP was initially described by Harbord *et al.* (1990) as 'an autosomal recessive neuronal migration defect with non-progressive cerebellar ataxia'. BFPP is a radiological diagnosis that consists of polymicrogyria characterized by multiple and fused small gyri, an irregular limit between white and grey matter, white matter abnormalities and cerebellar hypoplasia. Most of these features are also observed in cobblestone complex brain malformations formerly called type II lissencephaly (Barkovich, 1998), such as Fukuyama congenital muscular dystrophy and muscle-eye-brain disease (Piao *et al.*, 2005; Jissendi-Tchofo *et al.*, 2009), defined as cerebral cortical dysplasia combined with dysmyelination, severe dysplastic cerebellum with cysts and brainstem hypoplasia (Fukuyama *et al.*, 1981; Dobyns *et al.*, 1989; van der Knaap *et al.*, 1997; Barkovich *et al.*, 2005; Jissendi-Tchofo *et al.*, 2009).

A positional cloning approach localized a BFPP locus on chromosome 16q12.2–21 (Piao *et al.*, 2002; Chang *et al.*, 2003) and implicated the *GPR56* gene, which encodes an evolutionarily conserved dynamic G-protein-coupled receptor in the BFPP phenotype. Subsequently, Piao *et al.* (2005) demonstrated that *GPR56* mutations account for the majority of patients with typical BFPP. However, mutations in *GPR56* were not found in cases of bilateral frontoparietal polymicrogyria that lacked additional white matter or posterior fossa abnormalities nor in those with a more generalized polymicrogyria, indicating that the imaging changes seen in *GRP56*-related BFPP are specific (Piao *et al.*, 2005).

To date, 13 independent mutations in *GPR56* have been identified in 31 patients from 20 families (Piao *et al.*, 2004, 2005; Parrini, 2009). Functional studies of *GPR56* mutations that cause BFPP have suggested that they result in a loss of function attributable to aberrant processing and/or trafficking of the protein (Jin *et al.*, 2007; Ke *et al.*, 2007). Interestingly, *GPR56* mutations are located in different regions of the protein without any evidence of a relationship between the position of the mutation and phenotypic severity (Piao *et al.*, 2005).

Although *GPR56* ligands and downstream signalling pathways remain mostly unknown, studies of a *GPR56* knockout mouse model have shed light on the function of *GPR56* and the cellular defects underlying BFPP. The $GPR56^{-/-}$ phenotypes in the developing forebrain and rostral cerebellum share significant features, including abnormal neuronal positioning, rupture of the pial basement membrane and disorganization of the glial scaffold (Li *et al.*, 2008). At the forebrain level, loss of *GPR56* leads to a dysregulation of the maintenance of the pial basement membrane integrity that results in cortical lamination defects with overmigration through a defective basement membrane into the pial layer (Li *et al.*, 2008). More recently, analysis of the cerebellum of $GPR56^{-/-}$ mice showed that they display a severe malformation of the rostral cerebellum, reminiscent of cerebellar polymicrogyria, including the presence of ectopic granule cells, fusion of adjacent folia, disrupted layering of neurons and fragmentation of the pial membrane. These observations demonstrate that *GPR56* is also essential for normal morphogenesis of the rostral cerebellum (Koirala *et al.*, 2009). Altogether, studies of the *GPR56* knockout mouse model suggest that BFPP shares some features of the cobblestone brain malformation, but so far no human histopathological data have been documented.

To our knowledge, 31 patients with BFPP, aged from 13 months to 32 years, harbouring *GPR56* mutations have been described,

mostly originating from the Middle East or Indian subcontinent (Chang *et al.*, 2003; Piao *et al.*, 2004, 2005; Parrini *et al.*, 2009). Given the rarity of this malformation of cortical development, these patients were reported in three different series (of 12, 6 and 3 patients, respectively), making it difficult to compare phenotypes and to establish a comprehensive clinical spectrum that is representative of the phenotypic variability of *GPR56* BFPP. Reported clinical hallmarks consist of global developmental delay, abnormal eye movements with both strabismus and nystagmus, seizures and bilateral pyramidal and cerebellar signs (Piao *et al.*, 2004, 2005; Parrini *et al.*, 2009). Similarly, imaging studies emphasize a common and distinctive phenotype with bilateral symmetrical polymicrogyria most prominent in the frontoparietal regions with a decreasing antero-posterior gradient of severity, white matter signal changes and brainstem and cerebellar hypoplasia with little interindividual variability (Piao *et al.*, 2004, 2005; Parrini *et al.*, 2009). From the seminal description, bilateral patchy white matter signal changes were reported to be non-specific, but they could be considered a distinctive feature, given the lack of white matter changes reported in other polymicrogyria syndromes (Chang *et al.*, 2003). However, reports of the early clinical presentation and natural history, as well as age-related evolution of white matter changes, specifically MRI features at an early age, are scarce.

In light of the recent findings based on *GPR56*$^{-/-}$ animal model studies and the highlighted unanswered questions, the aim of this study is to provide a comprehensive overview of *GPR56*-related clinical and imaging phenotypes and their cobblestone-like features using a thorough analysis of a cohort of 14 patients, from eight different families with *GPR56* mutations that have not been previously described. Additionally, we report here the first description of a foetopathological case harbouring a *GPR56* mutation, further supporting the fact that *GPR56* BFPP is a 'cobblestone-like cerebral dysgenesis'. Finally, we searched for potential genotype–phenotype correlations and indicators that might predict the severity of the disorder.

Patients and methods

Patients

Thirty patients with bifrontoparietal polymicrogyria were referred to one of the two participating laboratories for molecular screening (APHP-Cochin Hospital and APHP Marseille). Of these, 20 were from consanguineous families with more than one family member affected and 10 were born to non-consanguineous families.

Informed consent was obtained from all patients according to national guidelines (Necker Enfants Malades University Hospital or local institutions). Patients were assessed clinically by at least one of the co-authors.

DNA mutation analysis

DNA was extracted from peripheral blood with the use of standard methods. All blood samples were obtained after confirmation of informed consent. DNA samples were screened for mutations in the 14 exons of the *GPR56* gene representing a coding region of 2079 bp (GenBank accession number AF 106858) from exon 2 to 14, using polymerase chain reaction amplification and direct sequencing. Primer sequences and polymerase chain reaction conditions are available upon request to the corresponding author. Sequencing reactions were carried out with the BigDye Terminator v1.1 Cycle Sequencing Kit (Applied Biosystems, Courtaboeuf, France) and loaded onto the ABI 3100 genetic analyser (PE Applied Biosystems, Foster City, USA).

Clinical information, brain magnetic resonance imaging analysis and grading of severity

Clinical information and brain MRI features of the 30 patients with BFPP were either collected directly at the Neuropaediatric unit of Necker Enfants Malades Hospital, Paris Descartes University, obtained from the referring physicians or sent by one of the authors and reviewed by N.B.B. and N.B.

MRI scans of the patients with *GPR56* mutations were retrospectively reviewed. After reviewing the images, the cases were classified according to the extent of polymicrogyria—predominantly frontoparietal or diffuse with an antero-posterior gradient. The degree of myelination of each patient was reviewed and compared with standards for the patient's age (Barkovich, 2005). White matter changes were classified according to the type of signal abnormality (i.e. patchy or diffuse) and the maximal location (periventricular or subcortical and anteriorly or posteriorly predominant). Ventriculomegaly was also noted.

The posterior fossa in each case was carefully reviewed with separate attention to the shape and size of the brainstem and pons. Cerebellar abnormalities were also noted, including vermian or hemispheric involvement, overall size, number of fissures and presence of cysts and their location, as previously described (Jissendi-Tchofo *et al.*, 2009). 'Hypoplasia' refers to a small vermis showing few or no fissures and no identifiable prepyramidal fissure, and 'dysplasia' refers to abnormal foliation or disorientation of fissures. The degree of involvement was further characterized as mild or severe based on consensus by the authors. According to the previous definition (Piao *et al.*, 2005), this analysis allowed us to define BFPP1 as typical bifrontoparietal polymicrogyria, with bilateral white matter signal changes, brainstem and cerebellar hypoplasia, and BFPP2 when these additional features were absent.

To assess the radiological differences between two possible locations of the mutation (extracellular domain versus transmembrane region), non-parametric statistical tests were used: the Wilcoxon test for continuous variables and the Fisher exact test for categorical variables (R software, http://www.R-project.org.).

Foetal case

A *GPR56* mutation was identified in a foetus presenting with an 'atypical lissencephaly with cerebellar hypoplasia', diagnosed prenatally at 35 weeks gestation, on ultrasonography and foetal MRI. In this case, the pregnancy was terminated for medical reasons at 35 weeks gestation, in accordance with French laws. Written consent for post-mortem and diagnostic studies was obtained from the parents. Neuropathological analysis was performed after fixation in a 10% formaldehyde solution containing NaCl (9 g/l) and $ZnSO_4$ (3 g/l) for six weeks. The brain was cut in a coronal plane and sections involving both hemispheres were embedded in paraffin. Paraffin blocks were cut at 8 μm. Sections were stained with haemalun-phloxin and cresyl violet-luxol-fast-blue (Klüver-Barrera). Immunohistochemical

Table 1 Clinical characteristics of the 14 individuals from eight families in whom a *GPR56* mutation was identified

Family	Gender/Age[a]	Head circumference	Cognitive delay	Motor delay	Dysconjugate gaze	Oromotor dyspraxia	Pyramidal signs	Cerebellar signs (ataxia)	Epilepsy	Age of onset	Type of seizure	Epileptic activity
I/1	M/31 years	<3rd percentile	Severe	Walking at 4 years	NR	Yes	Yes moderate spasticity	Severe	Yes	10 years	FS	Controlled (VPA PHT)
I/2	M/33 years	<3rd percentile	Severe	NA	NA	NA	Yes	Severe	Yes	NA	NA	Refractory
II/1	F/5 years	Normal	Severe	Walking at 2 years	Yes nystagmus	Yes	No	Severe	No			
II/2	M/9 years	Normal	Severe few words	Walking at 2 years	Yes nystagmus	Yes	Yes	Moderate	Yes	6 years	GTS/ At/Abs	Refractory (CBZ, VPA, CBZ)
III/1	M/5 years	Normal	Severe	Yes	Yes	No	No	Severe	Yes	2.5 years	FS GTCS	Controlled
IV/1	M/10 years	Normal	Severe	Walking at 4 years	NR	NR	Yes, left hemiplegia	Severe	Yes	3.5 years	GTCS	Refractory (VPA-TPM-CLB)
IV/2	M/20 years	Normal	Severe few words	Walking at 18 months	NA	NA	Yes	Severe	Yes	7 years	GTCS	Refractory
IV/3	M/18 months	Normal	Severe	Sitting without support	Convergent strabismus	No	Yes	Severe	No			
V/1	F/8.5 years	Normal	Severe	Walking at 5 years	Yes convergent strabismus	Yes	Yes	Moderate	Yes	2.5 years	GTCS	Controlled (VPA-LTG)
V/2	M/11 years	Normal	Severe few words	Walking at 5 years	Yes convergent strabismus	Yes drooling	Yes–no spasticity	Moderate	Yes	5 years	GTCS	Controlled (VPA)
VI/1	F/12 years	>98th percentile	Severe few words	Walking acquired but subsequently lost (11 years)	Yes convergent strabismus	Yes	Yes	Severe	Yes	8 years		Refractory
VII/1	F/8 years	Normal	Severe few words	Walking at 3 years	Yes convergent strabismus	Yes	No	Moderate	Yes	4 years	Abs	Controlled
VIII/1	F/7 years	Normal	Severe	Walking at 18 months	Yes	Yes	Yes	Severe	Yes	4 years 10 months	FS/GTS	Refractory
VIII/2	F/5 years	Normal	Severe	Walking at 22 months	Yes	Yes	NA	Severe	Yes	4.5 years	FS	Controlled

a Age at most recent follow-up.

Abs = atypical absence; At = atonic seizures; CBZ = Carbamazepine; F = female; FS = focal seizures; GTCS = generalized tonic clonic seizures; GTS = generalized tonic seizures; LTG = Lamotrigine; M = male; NA = information not available. PHT = Phenytoine; PMG = polymicrogyria; TPM = Topiramate; VPA = Valproate.

procedures were performed in areas selected after conventional histological study. Paraffin sections were immunostained for glial fibrillary acidic protein with a polyclonal antibody (1:200–1:400, DAKO, USA), MAP2 (1:100, HM2, SIGMA) and NeuN (1:500, MAB377, CHEMICON). The Universal Immunostaining System Streptavidin-Peroxydase Kit (Coulter) was used to reveal the reaction. Slides were incubated in citrate buffer at 98°C, placed in a microwave for 30 min, rinsed in distilled water, incubated in a 3% H_2O_2 solution for 5 min and then rinsed again in distilled water. After washing with phosphate buffered saline, they were treated with protein blocking agent for 5 min (100 µl/slide) at room temperature, without rinsing. The slides were then incubated with primary antibodies, diluted as specified above at room temperature for 60 min, and washed with phosphate buffered saline twice for 5 min each. Subsequently, they were incubated with biotinylated secondary antibody for 30 min at room temperature, washed with phosphate buffered saline twice for 5 min each and incubated in streptavidin-peroxidase complex for 45 min. After washing twice for 5 min in phosphate buffered saline, each slide was entirely covered with a freshly prepared 3,3′-diaminobenzidine-chromogen solution (100 µl/slide) for 5 min and finally rinsed with distilled water for 5 min. Haematoxylin was used to counterstain the brain sections. All sections were examined under a light microscope (Eclipse 800 NIKON) and some were selected for photographic documentation.

Results

From the 30 patients with bifrontoparietal polymicrogyria referred for molecular screening, 14 living patients and one foetal case were diagnosed as *GPR56*-related BFPP. There were six females and eight males, all from eight consanguineous families of Caucasian (four families), Middle Eastern (one family), Arab Mediterranean (one family), Iraqi (one family) and Turkish (one family) origin. The eight *GPR56* mutations identified in this study were novel and disrupted the protein at different levels, namely in the N-terminal domain: a frameshift mutation (p.E56RfsX24) and a missense mutation (p.C91Y), and in the mucin rich domain: one non-sense (p.Q123X) and one frameshift mutation (p.D224WfsX96). Additionally, two missense mutations were found in the transmembrane domain, TM1 (p.C418W) and TM3 (p.S485P), respectively, one frame deletion in TM2 (p.L449del) and one frameshift in TM2 (p.L406S406fsX41), but no mutation in the G-protein-coupled receptor proteolytic site cleavage site was found (Fig. 1).

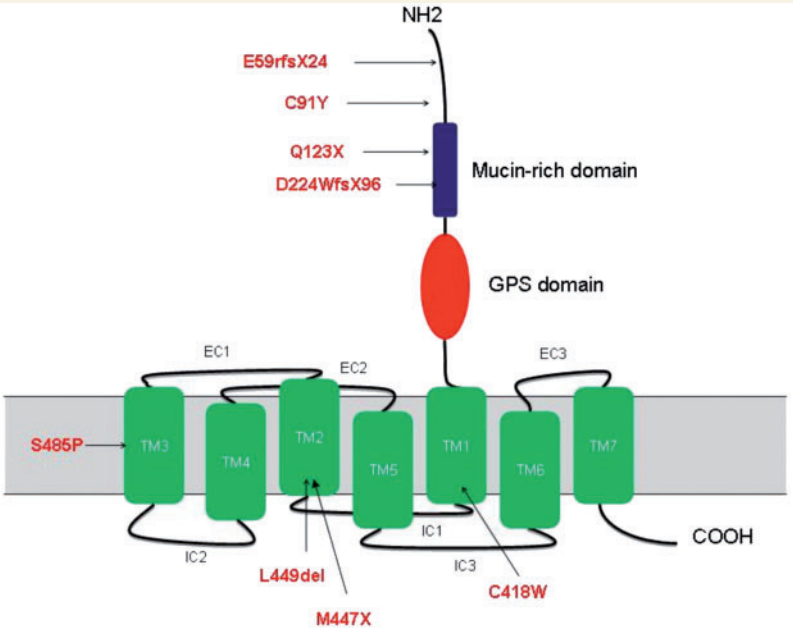
For the 15 patients in whom no *GPR56* mutation was found, 10 were from non-consanguineous families. All were severely mentally impaired, but none had a pseudomyopathic presentation at onset. Three had microcephaly. All had spastic tetraplegia without cerebellar signs. All patients had a phenotype consistent with BFPP2 on MRI, with bilateral polymicrogyria that predominated in both frontal lobes ($n = 7$) or a more diffuse picture with an antero-posterior gradient ($n = 3$). None of them had white matter or posterior fossa abnormalities.

Notably, half of the patients were tested for cytomegalovirus by analysis of urine and serology. The remaining patients were not tested, either because other siblings were similarly affected and harboured *GPR56* mutations (11/15 in patients with *GPR56* mutations, and 4/15 in patients without mutations) or because of the absence of clinical suspicion of cytomegalovirus, namely microcephaly (2/15 in patients with *GPR56* mutations and 3/15 in patients without mutations) and lack of intracranial calcification on CT scan.

Family V: from a foetal case with cobblestone lissencephaly to bifrontoparietal polymicrogyria

Among the mutations described above, one was identified in Family V, initially referred for genetic screening for unexplained cobblestone lissencephaly (Fig. 2A). The foetal case investigated was the 7th pregnancy (V/3) of a 40-year-old female who already had a healthy child. The parents were first cousin parents of Pakistani origin and had two children (V/1 and V/2), both affected by frontoparietal polymicrogyria. The mother had also had one previous miscarriage in Pakistan and two medical terminations of pregnancy. In two analysed cases, neuropathological studies showed diffuse cortical lesions associated with brain stem and cerebellar lesions characteristic of 'cobblestone' lissencephaly. No biological material was available for further molecular studies on these three foetuses. In view of the family history and imaging findings (cortical and cerebellar malformations), the pregnancy (V/3) was terminated at 35 weeks. Foetopathological examination showed no gross visceral, skeletal or ophthalmological malformations and normal brain biometric parameters. Macroscopic analysis of the brain showed complete agyria with cobblestone-like features on the cortical surface and vermian hypoplasia. At a microscopic level, coronal sections further disclosed disorganized cortical layers with a succession of normal, polymicrogyric and 'cobblestone-like' cortex (Fig. 2A–C). In addition to the cortical disorganization, immunohistochemical staining with NeuN and MAP2 antibodies showed ectopic neuronal overmigration through the pial basement membrane into the leptomeningeal space in unlayered regions (Fig. 2D). The corpus callosum and hippocampus were present and unaffected (Fig. 2E). There was agenesis of the cerebellar vermis and the cerebellar hemispheres were hypoplastic (Fig. 2F). Additionally, massive neuronal overmigration through the pial basement membrane was observed diffusely in the pons and focally in the cerebellar cortex (Fig. 2G). Muscle histopathology was normal and included α-dystroglycan analysis by immunostaining and western blot. In view of the suggestion of a cobblestone lissencephaly, mutational screening in *POMT1* and *POMT2* originally identified in the Walker–Warburg syndrome phenotype, was performed and was negative (Beltran-Valero de Bernabe *et al.*, 2002; van Reeuwijk *et al.*, 2005). Additional genetic testing of *POMGnT1*, *LARGE* and *Fukutin* genes was also negative.

We subsequently examined the two affected siblings (V/1 and V/2) with frontoparietal polymicrogyria, who presented with congenital hypotonia, cerebellar signs, strabismus and late onset generalized epilepsy. Since their clinical pattern was suggestive of *GPR56* BFPP, *GPR56* screening was performed and revealed a homozygous p.C418W mutation. This pathogenic mutation was also found in the foetus (V/3), demonstrating an association with the cobblestone complex (see also the 'Discussion' section).



Family	Case	Exon	Nucleotide change	Predicted amino acid change	Domain	Mutation type	Reference
I	1	3	c.174-175insC	E56RfsX24	N terminal	Frameshift	Novel
	2						
II	1	3	c. 272G>A	C91Y	N terminal	Missense	Novel
	2						
III	1	3	c.367c C>T	Q123X	Mucin rich domain	Nonsense	Novel
IV	1	5	c.671delA	D224WfsX96	Mucin rich domain	Frameshift	Novel
	2						
	3						
V	1	10	c.1254C>G	C418W	Transmemb (TM1)	Missense	Novel
	2						
	3						
VI	1	10	c.1215-1216delC	L406S406fsX41 (M447X)	Transmemb (TM2)	Frameshift	Novel
VII	1	11	c.1345delCTG	L449del	Transmemb (TM2)	In frame deletion	Novel
VIII	1	11	c.1453C>T	S485P	Transmemb (TM3)	Missense	Novel
	2						

Figure 1 Schematic representation of the *GPR56* protein and mutations in patients with BFPP. Identified mutations correspond to (i) three missense mutations: one at the tip of the N-terminus (p.C91Y), one in the first transmembrane domain (p.C418W) and one in the third transmembrane domain (p.S485P); (ii) one non-sense mutation, located in the mucin-rich domain (p.Q123X); (iii) two frameshift mutations located in the N-terminal domain (p.E59rfsX24) and in the mucin-rich domain (p.D224WfsX96) and (iv) one inframe deletion domain (p.L449del) and one frameshift mutation (p.M447X) in the second transmembrane domain. GPS = G protein-coupled receptor proteolytic site domain; EC = extracellular loop; IC = intracellular loop; TM = transmembrane domain.

Natural history of bilateral bifrontoparietal polymicrogyria: clinical features and clinical course

Detailed clinical information was available for eight males and six females (Table 1). Most patients presented before one year of age with severe hypotonia, pseudomyopathic behaviour and strabismus. Serum creatine kinase levels were normal in all cases. Four patients had a muscle biopsy prior to the diagnosis of BFPP and histochemistry was normal. All patients made motor progress. At the last evaluation (age ranging from 1.5 to 33 years, median 8.25 years), all patients except one (an 18-month-old male IV/3) were able to walk unaided but with moderate to severe ataxia. Age of ambulation ranged from 1.5 to 5 years (median 2.5 years).

All patients had severe mental retardation and communication skills limited to eye contact and a few isolated words. Head circumference was normal in 11/14 patients. The two oldest

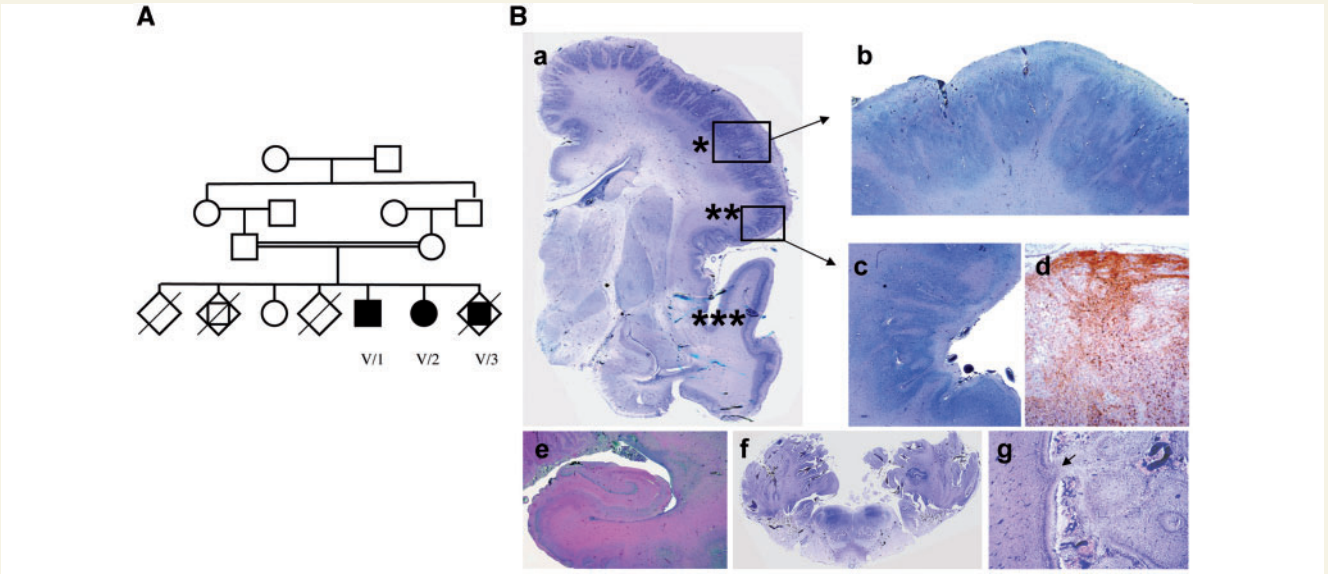


Figure 2 (**A**) Pedigree of the family carrying the p.C418W *GPR56* mutation reported in this study. Square = male; round = female; diamond = foetus. Black square or round = affected person. (**B**) Neuropathological analysis of foetus V/3 that carried a p.C418W *GPR56* mutation. (a) Coronal section of the left cortical hemisphere revealed the succession of cobblestone-like (*), polymicrogyric (**) and normal cortex (***) in a same brain section. (b and c) Details of the cobblestone and polymicrogyric unlayered cortex are illustrated in b and c, respectively. (d) Neurospecific MAP2 immunostaining on the cortical section of the foetus at 35 weeks of gestation showed the presence of numerous neuronal cells clusters beyond the basement membranes, in the meninges. (e) The folding and architecture of the hippocampus stained by Nissl is normal. (f) Microscopic analyses of the cerebellum revealed a simplification of the cerebellar lobules and a vermian agenesis. (g) The same overmigration though the pial basement membrane were observed focally in the cerebellar cortex.

patients were microcephalic (I/1 and I/2) and Patient VII/1 had macrocephaly in association with hydrocephalus. All patients had pyramidal signs with brisk deep tendon reflex but without spasticity. Abnormal eye movements were also found in all cases consisting of nystagmus or strabismus but no other ocular abnormalities were detected.

Epilepsy affected 12/14 patients with onset ranging from 2.5 to 10 years of life (median 4.65 years) and mainly consisted of generalized seizures, either tonic clonic or atypical absences. The two unaffected patients were younger, aged 18 months and 5 years at the time of evaluation. Two patients presented with partial status epilepticus. Six patients had a few seizures initially, but were then seizure-free for 2 years following antiepileptic drug adjustments. Six patients had medically refractory seizures.

None of the patients had normal EEG background activity or normal posterior α-rhythms on eye closure. Only interictal EEG recordings were obtained. The most common EEG pattern consisted either of bursts of fast activity in the frontocentral regions ($n = 5$) (Fig. 3) or more diffuse notched θ sharp waves and spikes and waves discharges. In four cases, there were subclinical runs of high amplitude sharp and slow wave complexes mixed with high amplitude α-activity. This activity was more prominent over bilateral frontal and temporal areas.

Altogether, this follow-up study indicates that the 14 patients with *GPR56* mutations were phenotypically homogeneous with pronounced early central hypotonia and cerebellar signs, later evolving to share common clinical features with some variability in the epilepsy phenotype but similar interictal EEG abnormalities.

Neuroimaging findings

Neuroimaging features of the 14 patients with *GPR56* mutations were re-examined. In total, 13 MRIs were analysed and consecutive images were obtained for two patients. Magnetic resonance data are detailed in Table 2.

First, we examined the hallmark of BFPP, i.e. bilateral polymicrogyria with anterior to posterior gradient. The characteristic pattern of bilateral and symmetrical polymicrogyria with a slightly thickened cortex with shallow sulci and irregular grey–white matter interface was observed in all cases. We further classified the extent of the symmetrical polymicrogyria into two categories, involving the fronto-parietal lobes ($n = 4$) or generalized with an anterior to posterior gradient ($n = 9$) (Fig. 4).

To further assess the presence of cobblestone-like signs (Jissendi-Tchofo *et al.*, 2009), we examined the cerebellum, the brainstem and white matter evolution. Interestingly, all 13 patients showed moderate to severe cerebellar dysplasia with subpial and cortical cysts and vermian disorganization affecting the superior vermis (11/13) or involving the whole vermis (2/13). Additionally, 5/14 patients also demonstrated hemispheric cerebellar dysplasia with surrounding cysts closely located in the peripheral hemispheres (Fig. 5). There was no obvious relationship between the extent and type of cerebral and cerebellar abnormalities. At the brainstem level, hypoplasia with flattening of the ventral portion of the pons at the level of the middle cerebellar peduncle was detected in all patients (Fig. 6). In the most abnormal scans (Table 2, Patients IV/3, V/1, V/2 and VII/1), the brainstem had an unusual posterior concavity to the posterior aspect.

Table 2 Radiological features of our new *GPR56* patients

Family/ case	Gender/age at MRI	Polymicrogyria distribution	Lateral ventricles	White matter abnormalities	Corpus callosum	Cerebellar vermis		Cerebellar hemispheres		Brainstem
						Dysplasia	Cyst	Dysplasia	Cyst	
I/1	M/28 years	Frontoparietal	Enlarged	Patchy periventricular predominance	Thin and body arched	Superior and median vermis	+	–	+	Hypoplastic pons
I/2	M/33 years	NA	NA	NA	NA	NA	NA	NA	NA	NA
II/1	F/5 years	Frontoparietal	Slightly enlarged	Patchy	Thin	Superior vermis	+	–	+	Hypoplastic pons
II/2	M/8 years	Frontoparietal	Slightly enlarged	Patchy periventricular and frontal predominance	Thin	Superior vermis	+ (sup)	–	+	Hypoplastic pons Cyst in the ventral pons
III/1	M/3 years	Frontoparietal	Slightly enlarged	Patchy periventricular and frontal predominance	Normal	Superior vermis	+ (sup)	–	+	Hypoplastic pons Cyst in the ventral pons
IV/1	M/10 years	Diffuse max fronto-parietal Right sided lentiform nucleus infarct	Enlarged	Patchy periventricular and frontal predominance	Thin	Superior vermis	+	–	+	Hypoplastic pons
IV/2	M/20 years	Diffuse max frontoparietal	Enlarged	Patchy periventricular and frontal predominance	Thin	Superior vermis	+	–	+	Hypoplastic pons
IV/3	M/4 months	Diffuse max frontoparietal	Enlarged	Diffuse	Thin	Superior vermis	+	+	+	Hypoplastic pons
	M/18 months	Diffuse max frontoparietal	Enlarged	Patchy with subcortical and frontal predominance	Thin and body arched	Superior vermis	+	+	+	Severely Hypoplastic pons with posterior concavity
V/1	F /4 months	Diffuse max frontoparietal	Enlarged	Diffuse	Thin	Superior vermis	+	+	+ (sup)	Hypoplastic pons
	F/8 years	Diffuse max frontoparietal	Enlarged	Patchy with subcortical and frontal predominance Reduced volume	Thin and body arched	Superior vermis	+	+	+ (sup)	Severely hypoplastic pons with posterior concavity Cyst in the ventral pons
V/2	M/2 years	Diffuse max frontoparietal	Enlarged	Patchy	Thin and body arched	Superior and median vermis	+	+	+ (sup)	Hypoplastic pons
	M/11 years	Diffuse max frontoparietal	Enlarged	Patchy with subcortical and frontal predominance	Thin and body arched	Superior and median vermis	+	+	+	Severely hypoplastic pons with posterior concavity Cyst in the ventral pons
VI/1	F/12 years	Diffuse max frontoparietal	Enlarged	Patchy	Thin and body arched	Superior vermis	+	+	+	Hypoplastic pons
VII/1	F/20 months	Diffuse max frontoparietal	Enlarged	Patchy with subcortical predominance	Thin and body arched	Superior vermis (mild)	+	+ (sup)	+	Severely hypoplastic pons with posterior concavity
VIII/1	F/5 years	Diffuse max frontoparietal	Slightly enlarged	Patchy with subcortical and frontal predominance	Thin	Superior vermis	+	–	+	Hypoplastic pons
VIII/2	F/ 7 years	Diffuse max frontoparietal	Slightly enlarged	Patchy with subcortical and frontal predominance	Thin	Superior vermis	+	–	+	Hypoplastic pons

White matter signal changes were determined in T_2/fluid attenuation inversion recovery sequence, and classified as patchy when confluent signal changes, or diffuse.
+ = present; – = absent; NA = not-assessed when images were insufficient for reviewing; sup = superior.

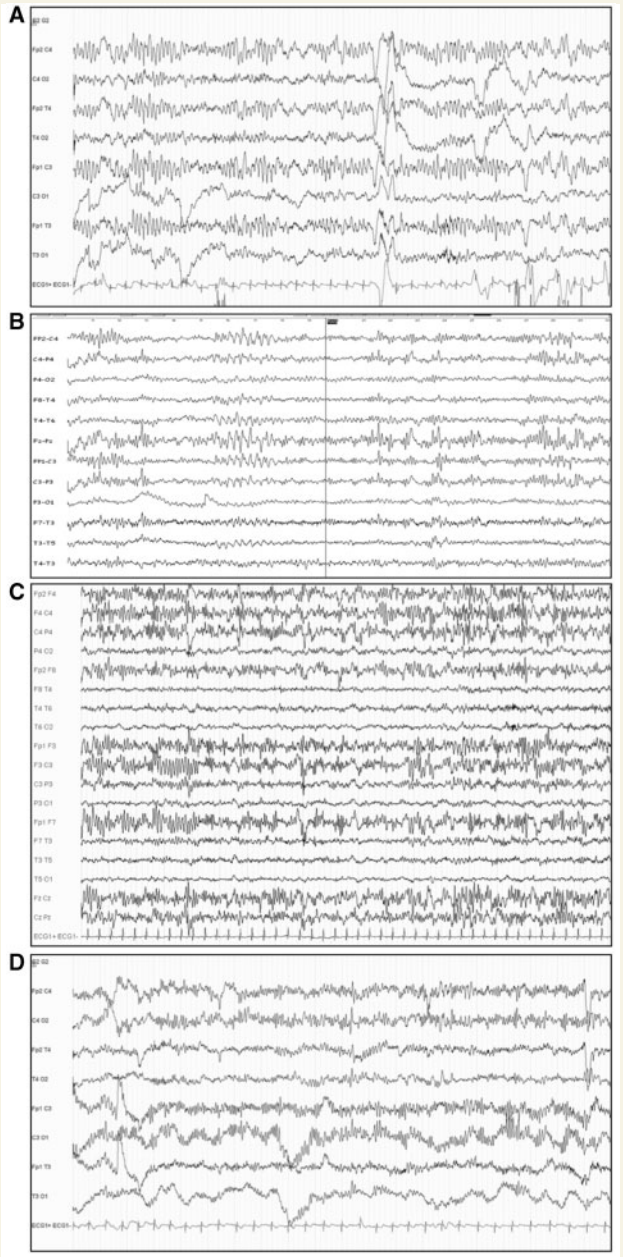


Figure 3 Representative interictal electroencephalogram pattern in patients with *GPR56* BFPP. (**A**) Theta activity with medium amplitude and rare and brief spike and wave discharges with predominance in both frontal and temporal areas (Patient II/1 aged 9 years) (Patient V/2 aged 8 years). (**B**) Runs of fast activity in frontocentral regions resembling α-like activity with high amplitude theta activity maximal in frontal and central regions (Patient II/1 aged 9 years). (**C**) Diffuse delta waves (2–3 Hz) intermixed with α-like activity and high voltage with paroxysmal discharges of spike and waves, maximal in both frontal and temporal areas (Patient VIII/2 aged 5 years). (**D**) Unusual α-like activity over both frontal regions (Patient V/1 aged 10 years). No physiological sleep pattern. Amplitude 10 μV/mm. Speed 15 mm/s.

Of note, none of these patients had evidence of severe brainstem dysplasia, which is one of the characteristic features of cobblestone complex lissencephaly.

Moreover, all patients with *GPR56* mutations exhibited patchy T_2 high signal white matter signal abnormalities to a greater or lesser extent, suggestive of dysmyelination and reminiscent of cobblestone-like lissencephalies (Fig. 7). In two patients (IV/3 and V/2), successive MRIs allowed us to follow the progression of myelination. In both, the white matter abnormalities showed a peculiar pattern of evolution with a severe hypomyelination pattern at four months that evolved into patchy white matter signal abnormalities later in childhood (Fig. 8). Strikingly, the evolution of the abnormal white matter signal began in the parieto-occipital subcortical region, which is in contrast to the normal centrifugal pattern of myelination.

Additional significant magnetic resonance changes in patients with *GPR56* mutations consisted of a thin corpus callosum with absent rostrum, often with a smoothly arched callosal body and an enlarged subarachnoid space with ventriculomegaly ($n = 8$).

Taken as a whole, these observations collectively demonstrate that *GPR56*-related BFPP is a cobblestone-like 'polymicrogyria' that combines anteriorly predominant polymicrogyria and cerebellar vermian dysplasia with subpial and cortical cysts, and to a lesser extent cerebellar hemispheric dysplasia with cysts.

GPR56 mutations: influence of mutation on the severity of *GPR56* bilateral bifrontoparietal polymicrogyria

Based on previous functional studies demonstrating that BFPP-causing mutations impair protein trafficking and cell surface expression to varying degrees according to their location (Jin *et al.*, 2007), and in light of the interindividual variability observed in our study, we analysed the influence of the position of the mutation and type of substitution on the clinical and radiological features (Table 3). Although some discrepancies were observed between patients with mutations in the N-terminal domain (i.e. extracellular domain) and transmembrane spanning domains, notably on the severity of epilepsy (age of seizure onset and drug resistance), as well as the extent of polymicrogyria and white matter abnormalities, no statistical differences were found. The less severely affected patients harboured mutations in the N-terminal domain, which is of interest because biochemical results suggest that these mutations result in more drastic functional consequences on *GPR56* function, i.e. reduced intracellular trafficking and poor cell surface expression (Jin *et al.*, 2007).

Discussion

The aim of our analysis was to provide new insights into the phenotype of *GPR56* BFPP (OMIM® 606854) in light of recent data from animal studies demonstrating that loss of GPR56 results in cobblestone cortex and leads to rostral cerebellar dysplasia. Combined with the first foetopathological case with a *GPR56* mutation, our study examined the clinical and brain MRI

Table 3 Comparison of clinical and radiological features between patients with *GPR56* BFPP with mutations in the extracellular domain and mutations in the transmembrane domain

	Extracellular domain[a]	Transmembrane domain[a]	*P*-value[b]
Total patients (*n*)	8	6	
Median age in years (range)	9.5 (1.5–33)	8.25 (5–12)	0.75
Severe mental retardation (%)	8/8 (100)	6/6 (100)	1
Ability to walk (%)	6/7 (85.7)	5/6 (83.3)	1
Dysconjugate gaze (%)	4/4 (100)	6/6 (100)	1
Epilepsy (%)	6/8 (75)	6/6 (100)	0.47
Median age of seizure onset in years (range)	6 (2.5–10)	4.65 (2.5–8)	0.71
Refractory epilepsy (%)	4/8 (50)	2/5 (40)	1
MRI (*n*)	7	6	
Diffuse polymicrogyria (%)	3/7 (42.8)	6/6 (100)	0.07
Enlarged ventricles (%)	4/7 (51.1)	4/6 (66.7)	1
Patchy white matter abnormalities (%)	3/7 (42.8)	5/6 (83.3)	0.27
Vermian and hemispheric dysplasia (%)	1/7 (14.3)	4/6 (66.7)	0.10
Vermian and hemispheric cyst (%)	7/7 (100)	5/6 (83.3)	0.46
Brainstem hypoplasia (%)	7/7 (100)	6/6 (100)	1

a The denominator indicates the number of patients for whom specific information was available.
b To assess the differences between defined groups of patients and to evaluate the correlation with the location of the mutation (extracellular domain versus transmembrane mutation) between the severity of cortical dysgenesis and pontocerebellar abnormalities, non-parametric statistical tests were used [Kruskal–Wallis test for multiple group comparison and χ^2 McNemar test (Statistica version 7.1, StatSoft France, 2005, www.statsoft.fr)]. $P<0.05$ was considered significant.

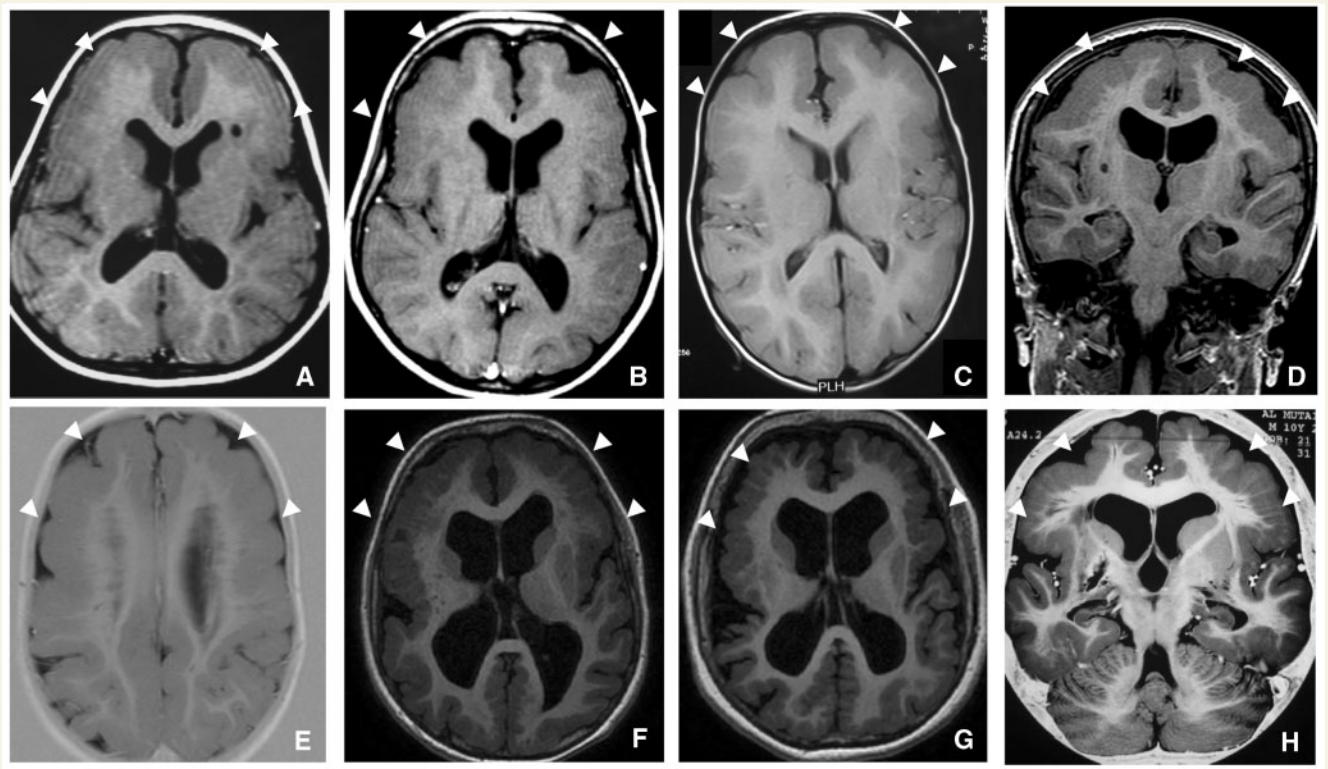


Figure 4 Representative brain magnetic resonance images of patients with *GPR56* BFPP. T_1-weighted axial section of Patient II/1 (8 years at MRI, **A**), Patient II/2 (5 years at MRI, **B**), Patient III/1 (3 years at MRI, **C**), Patient VIII/1 (7 years at MRI, **E**), Patient V/1 (8 years at MRI, **F**), Patient V/2 at 7 years (11 years at MRI, **G**) and T1-weighted coronal section of Patient II/2 (5 years at MRI, **D**) and Patient IV/1 (10 years at MRI, **H**). These images demonstrate different degrees and extent of polymicrogyria involving the frontoparietal regions bilaterally (**A–C**), or more generalized polymicrogyria with frontoparietal predominance (**E–G**). Coronal sections (**D** and **H**) at the level of the hippocampus show the parietal predominance of polymicrogyria and the relative preservation of the temporal lobes. Note the ventricular size that is either not (**C**), moderately (**A** and **B**) or severely enlarged (**E–H**). Note also the right sided lentiform nucleus infarct in Patient IV/1 (**H**).

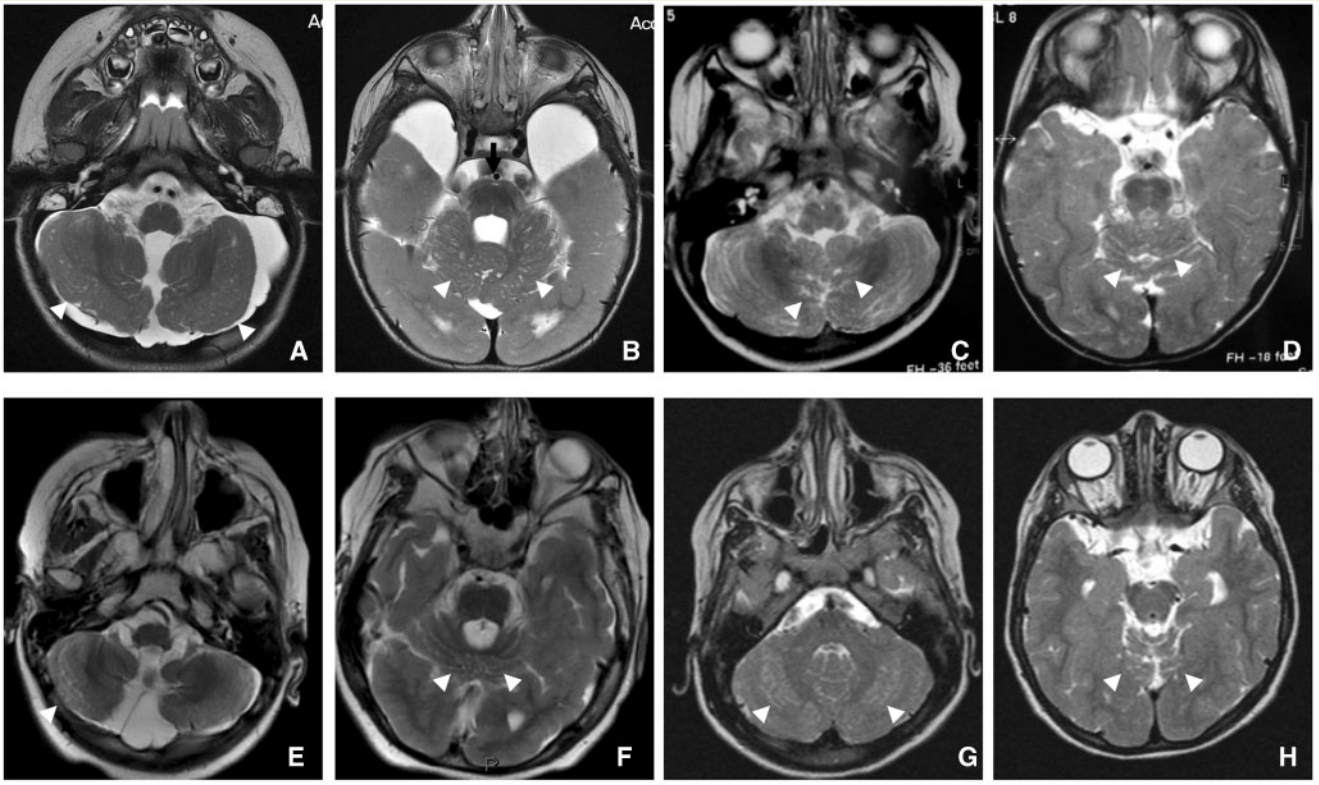


Figure 5 Representative T_2-weighted axial sections showing the different features of cerebellar hypoplasia and dysplasia in *GPR56* BFPP. These images demonstrate multiple cysts located in dysplasic cerebellar hemispheres (**A**, **C**, **E** and **G**) and in the cerebellar vermis (**B**, **D**, **F** and **H**). Different degrees of severity considered as severe cerebellar dysplasia and brainstem hypoplasia in Patient IV/3 (18 months at MRI, **A** and **B**) and Patient VII/1 (20 months at MRI, **C** and **D**), and milder severity in Patient V/2 (11 years at MRI, **E** and **F**) and Patient II/2 (5 years at MRI, **G** and **H**). Note the small pons with overmigration (**B**, Patient IV/3, 18 months at MRI). There is an exaggerated rounded appearance to the high signal myelinated corticospinal tracts (thin black arrows). There are several cerebellar cysts (thick black arrow).

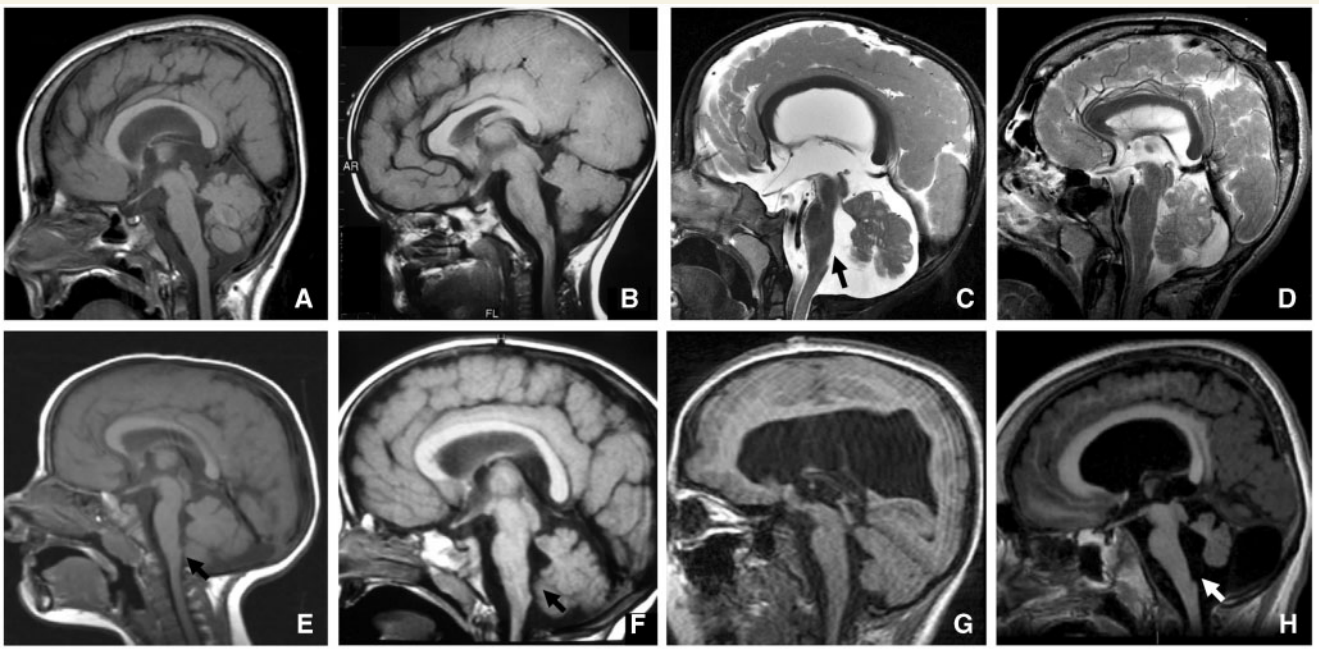


Figure 6 Representative T_1-weighted midline sagittal images in *GPR56* BFPP. In the sagittal plane, the pons is thinned with either a flat aspect (**A**, Patient II/2), (**B**, Patient III/1), (**D**, Patient IV/1) (**G**, Patient VI/1), and in the most severe form, a concave posterior border (**C**, Patient IV/3), (**E**, Patient VIII/1) (**F**, Patient VII/1), (**H**, Patient V/2), and the midbrain tectum is abnormally large. Note the different aspect of corpus callosum ranging from normal (**B**) to hypoplasia thin splenium and arched body (**C** and **H**).

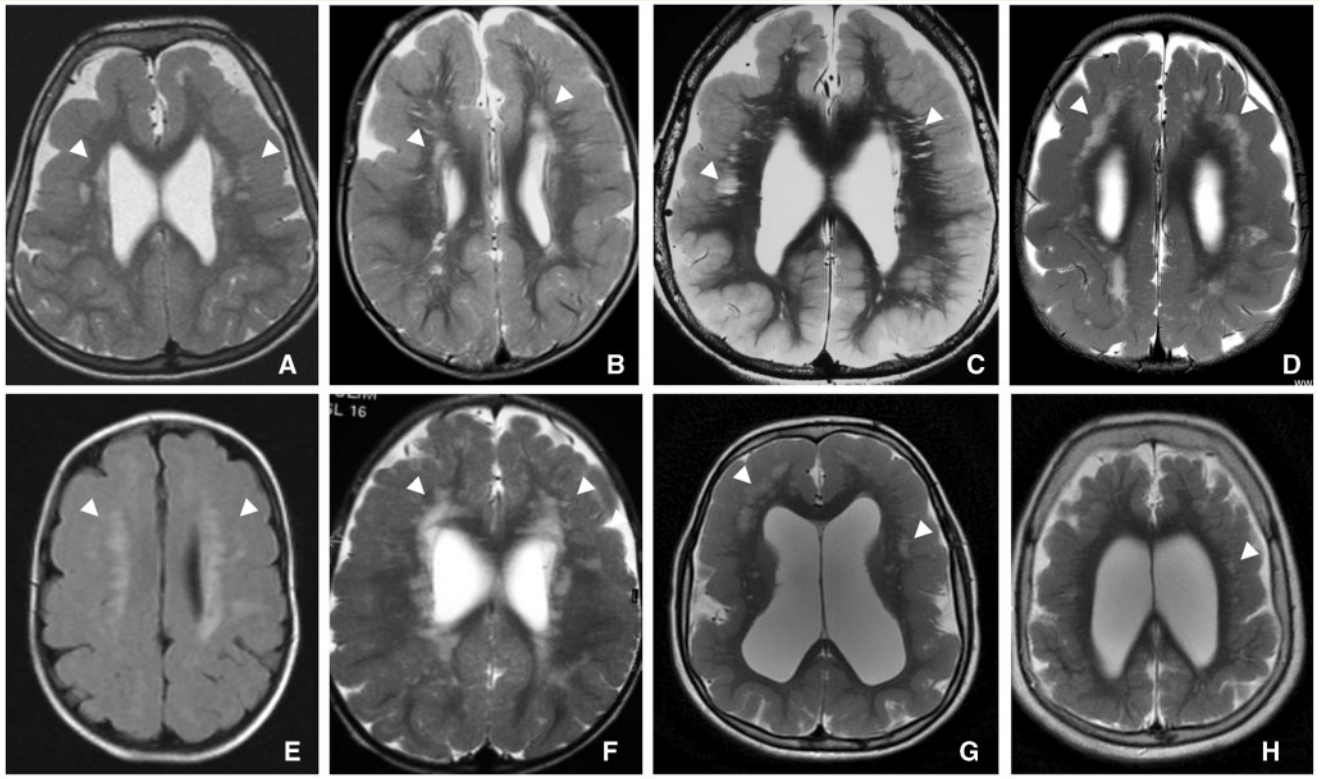


Figure 7 Representative axial T_2 images in *GPR56* BFPP. These images demonstrate polymicrogyria in the frontoparietal regions bilaterally, as well as patchy bilateral signal change in the white matter, patchy (**A**, Patient II/1), (**D**, Patient IV/3), (**E**, Patient V/1), (**F**, Patient VI/1) (**G**, Patient VII/1) or spotty periventricular and frontal (**B**, Patient III/1), (**C**, Patient IV/1) (**H**, Patient V/2).

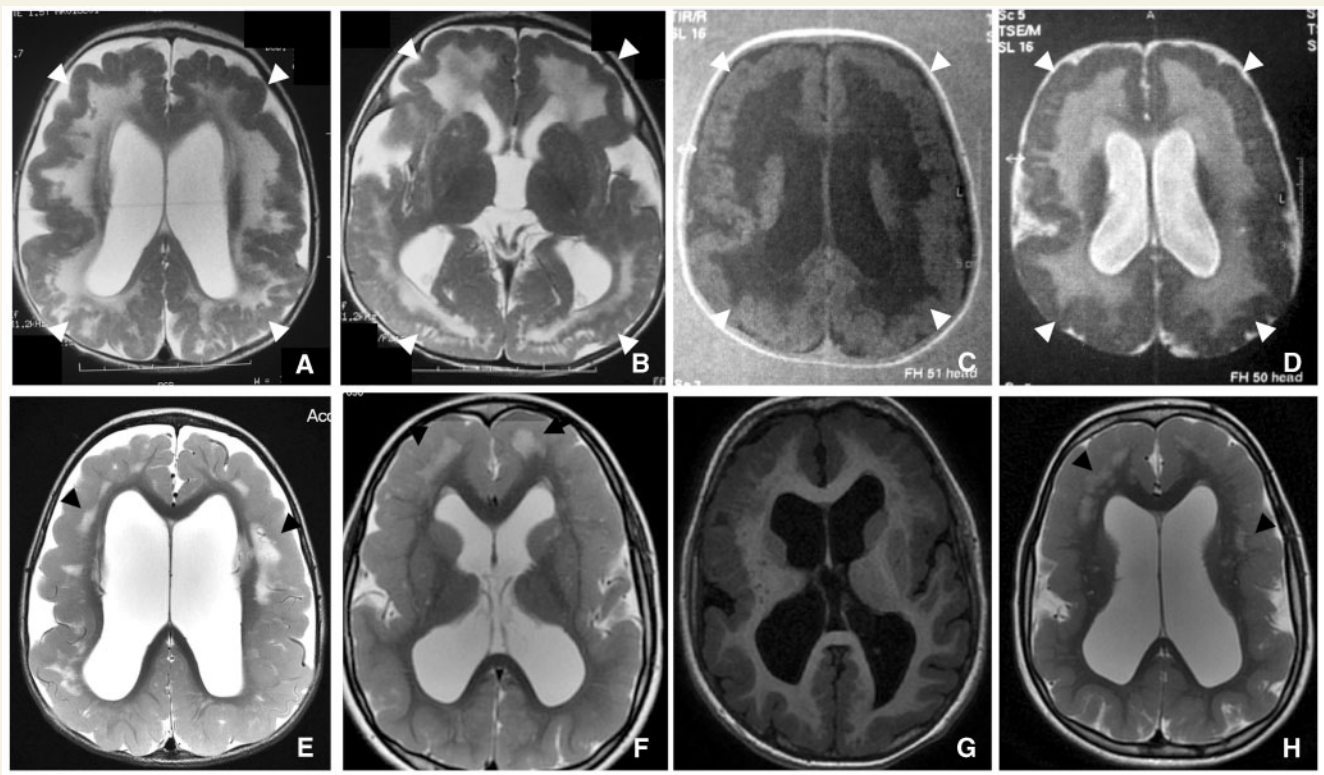


Figure 8 Axial T_2 images of Patient IV/3 (**A**, **B**, **E** and **F**) and Patient V/2 (**C**, **D**, **G** and **H**) showing the appearance of the white matter at 4 months (**A–D**), highly suggestive of severe hypomyelination and the subsequent evolution to patchy signal changes mostly prominent in subcortical and frontal regions [at the age of 18 months in Patient IV/3 (**E** and **F**) and 9 years in Patient V/2 (**G** and **H**)].

characteristics of 14 individuals with BFPP from eight families harbouring eight novel mutations in the *GPR56* gene. The overall information that can be drawn from this study is that the range of central nervous system involvement is wider than originally described and that cortical, white matter as well as cerebellar involvement occurs in BFPP and is highly reminiscent of cobblestone complex lissencephaly (Barkovich, 1998).

Taken together, the clinical and radiological findings described in our study in combination with previously reported data, suggest that *GRP56* defects produce a 'cobblestone-like cortical dysgenesis'.

GPR56 bilateral bifrontoparietal polymicrogyria: a peculiar course with a pseudomyopathic presentation that subsequently evolves into severe mental and motor retardation with generalized epilepsy

The overwhelming majority of patients presented in the first months of life with severe hypotonia and a pseudomyopathic presentation. At first, clinicians suspected congenital muscular dystrophies and performed muscle biopsies that were normal. Subsequently, central hypotonia became more obvious. Later in infancy, patients exhibited clinical features consistent with a developmental brain malformation including severe mental and motor retardation and pyramidal signs, and in addition developed cerebellar signs and eye movement abnormalities. This clinical presentation appears to be specific to *GPR56*-related BFPP and should lead clinicians who initially suspect congenital muscular dystrophy (Piao *et al.*, 2002, 2005; Chang *et al.*, 2003) to also consider the diagnosis of a *GPR56*-related disorder.

Epilepsy is a consistent feature in *GPR56* BFPP and mainly consists of generalized seizures, either tonic clonic or atypical absences with an EEG pattern highly reminiscent of those with lissencephaly (Piao *et al.*, 2005; Parrini *et al.*, 2009). Notably we provide the first detailed description of the interictal EEG pattern in *GPR56* BFPP and highlight the similarity with the pattern seen in diffuse cortical malformations typically described in type I lissencephaly (Gastaut *et al.*, 1987; de Rijk-van Andel *et al.*, 1988; Santanelli, 1991; Mori *et al.*, 1994; Raymond *et al.*, 1995). This consists of unusual α-like activity of low amplitude and is not modified by eye opening or closure. The unusual fast activity often persists as the child gets older and is later associated with high amplitude sharp and slow wave complexes mainly in the frontal and temporal regions bilaterally (Parrini *et al.*, 2009). This pattern is helpful in detecting neuronal migration disorders and, in some cases, may contribute to predicting the timing of seizure onset in the first few years of life. According to Dalla Bernardina and colleagues (1996), the earlier both the high amplitude and fast activity appear, combined with their generalized appearance, the greater the probability of early seizure onset. In our series, EEGs were performed at the age of seizure onset and further studies are therefore needed to evaluate the predictive value of early seizure onset in *GPR56* BFPP.

Further evidence suggesting that *GPR56* bilateral bifrontoparietal polymicrogyria is a 'cobblestone-like cortical dysgenesis'

Previous studies have highlighted the occurrence of white matter lesions combined with polymicrogyria in *GPR56* BFPP. White matter changes are rare in other polymicrogyria syndromes i.e. frontal, perisylvian or generalized polymicrogyria (Jansen and Andermann, 2005; Piao *et al.*, 2005). By contrast, they are common findings in cobblestone complex lissencephalies (Barkovich, 1998). Thus it is not surprising that BFPP had previously been termed 'cobblestone lissencephaly with normal eyes and muscle' (Barkovich, 1996).

Cobblestone lissencephaly encompasses a large group of neuronal migration disorders resulting from overmigration of neurons beyond the developing cerebral cortex, passing through defects of the glia limitans into the subarachnoid space. This aberrant migration produces irregular neuronal 'cobblestones' (ectopia) on the surface of the brain and is a feature of three distinct human disorders of varying severity: Walker–Warburg syndrome (most severe); muscle-eye-brain disease and Fukuyama congenital muscular dystrophy (least severe) (Brockington *et al.*, 2005; Mercuri *et al.*, 2006, 2009; Godfrey *et al.*, 2007). These three disorders are characterized by cerebral cortical dysplasia that ranges from pachygyria to agyria, combined with dysmyelination, severe dysplastic cerebellum with cysts and brainstem hypoplasia (Fukuyama *et al.*, 1981; Dobyns *et al.*, 1989; van der Knaap *et al.*, 1997; Barkovich *et al.*, 2005; Jissendi-Tchofo *et al.*, 2009).

This is the first study to our knowledge, which provides evidence that *GPR56*-related BFPP and cobblestone lissencephaly share additional specific features, which consist of cerebellar dysplasia with cysts and severe hypomyelination that subsequently evolves to patchy dysmyelination, and overmigration of neuronal cells in the leptomeningeal space.

First, we show that hind and midbrain abnormalities are consistent key features in *GPR56* BFPP. While previous reports described only cerebellar hypoplasia (Piao *et al.*, 2005), we found a high rate of cerebellar dysplasia with microcysts. Vermian dysplasia and cysts strongly predominate in the superior vermis and are observed in >90% of patients in this study, regardless of age. Of note, the dysplasia can be more diffuse involving the whole vermis and the hemisphere. However, no obvious relationship between the extent or type of cerebral and cerebellar abnormalities were found. Hence, cerebellar vermian dysplasia with accompanying cysts is an important finding in BFPP, since it can be recognized more readily than cortical polymicrogyria in a young infant and should prompt a careful search for *GPR56* mutations.

Second, combined with previous reports that highlighted the importance of white matter abnormalities in *GPR56* BFPP, our observations have allowed us to demonstrate that the myelination process is also impaired in *GPR56* BFPP. White matter abnormalities are maximal at a young age and consist of severe and diffuse hypomyelination, but myelination does progress, albeit in an unusual manner proceeding from the peripheral subcortical region

Table 4 Characteristics of *GPR56* bifrontoparietal polymicrogyria compared with congenital muscular dystrophy

Disorder	Role	Clinical presentation	Cerebral cortex	Cerebellar cortex	White matter	Brainstem	Ocular anomalies
GPR56 BFPP	*GPR56* acts as a G-protein-coupled receptor that localizes to radial glial foot processes directly adjacent to the pial basement membrane and is required to maintain structural integrity of this basement membrane	Hypotonia; delayed motor; delayed cognition; variable seizures; normal CK	Frontoparietal polymicrogyria Diffuse PMG with antero-posterior gradient	Polymicrogyria with or without cysts	Delayed myelination in cerebrum	Pontine hypoplasia	Abnormal eye movements
Fukuyama congenital muscular dystrophy (Fukuyama type and similars)	Mutation in the gene encoding *fukutin* that probably participates in the biosynthesis pathway of dystroglycan, involved in the binding activity for the ligand laminin	Hypotonia; delayed motor; delayed cognition; variable hydrocephalus; variable seizures; variable CK	Frontal polymicrogyria; temporo-occipital cobblestone cortex with irregular inner surface and smooth outer surface	Polymicrogyria with or without cysts	Delayed myelination in cerebrum; peripheral white matter myelinates first	Variable pontine hypoplasia; variable fused colliculi	Abnormal eye movements; myopia; cataracts; retinal 'round' lesions
Muscle-eye-brain disease	Mutation in O-mannose β-1,2-*N* acetylglutaminyltransferase (*POMGTnT1*) that participates in O mannosyl-glycan synthesis, results in disorder of radial migration and disruption of the pial barrier	Hypotonia; delayed motor; ocular anomalies; variable hydrocephalus; variable seizures; normal CK	Diffusely dysplastic, same features but intermediate severity between Fukuyama congenital muscular dystrophy and Walker-Warburg syndrome	Polymicrogyria with or without cysts; vermian hypogenesis	Patchy T_1 and T_2 prolongation; variable callosal hypogenesis	Pontine hypoplasia; fused colliculi	Abnormal eye movements; myopia; glaucoma; cataracts; retinal dysplasia; hypoplastic nerve
Walker–Warburg syndrome	Gene encoding O-mannosyl transferase (*POMT1*) involved in O-mannose-linked glycosylation of proteins important for the formation of glia limitans	Hypotonia; no motor milestones; no cognition; ocular anomalies; hydrocephalus; variable seizures; normal CK	Diffuse cobblestone cortex; hydrocephalus	Polymicrogyria with or without cysts; variable cephalocele	Leucodystrophy; variable callosal hypogenesis	Severe brainstem hypoplasia; fused colliculi; mid-hindbrain junction dorsal kink	Anterior chamber and iris anomalies; microphthalmos; cataracts; colobomas; retinal dysplasia and detachment
Congenital Muscular Dystrophy Merosin deficiency	Mutation in the laminin α2 gene (*LAMA2*), is a permissive substrate for migration of oligodendrocyte precursors	Hypotonia; delayed motor; high CK	Occipital agyria (no cobblestone cortex)	Polymicrogyria with or without cysts	Striking leucodystrophy involving U fibres	Mild pontine hypoplasia	None

CK = serum creatine kinase.

centrally, which is the reverse of normal myelination process. These changes are strikingly similar to those seen in Fukuyama congenital muscular dystrophy (Dobyns *et al.*, 1989; Aihara *et al.*, 1992; Valanne *et al.*, 1994; Barkovich, 1998). Their exact nature is unknown but abnormal production or migration of oligodendrocytes in *GPR56* BFPP cannot be excluded. This raises the possibility that delayed myelination and dysmyelination in *GPR56* mutations might result in abnormal axonal pathfinding.

Thirdly, foetopathological features reported here, demonstrate that *GPR56* mutations lead to a cobblestone-like brain malformation with succession of normal, polymicrogyric and 'cobblestone-like' cortex, with focuses of ectopic neuronal overmigration through the pial basement membrane into the leptomeningeal space in unlayered regions, combined with massive neuronal overmigration in the pons and focally in the cerebellar cortex.

In view of these findings and to further investigate whether cobblestone lissencephaly and *GPR56* BFPP share additional features, we compared other brain structures (Table 4). At the forebrain level, the main difference is the primary location and the gradient of cortical dysplasia that predominates in the temporo-occipital region in Fukuyama congenital muscular dystrophy compared with the frontoparietal gradient seen in *GPR56* BFPP. In the midbrain and hindbrain, the cerebellum is more severely hypoplastic in cobblestone lissencephaly than in BFPP, where the cerebellar hemisphere is dysplastic and combined with cysts. In the brainstem, pontine midline cleft and deformity of the mid-hindbrain junction (pontomedullary 'kink'), which is a hallmark of cobblestone lissencephaly, was not observed in *GPR56* BFPP. These features are remarkably predominant in the cobblestone lissencephaly groups, differentiating them from patients with *GPR56* BFPP. These differences might reflect the distinctive pathophysiological mechanisms of both conditions.

GPR56 bilateral bifrontoparietal polymicrogyria a 'cobblestone-like cortical dysgenesis': pathophysiological similarities with cobblestone lissencephalies

Neuronal migration disorders are related to the impairment of several genetically determined processes that act either at the beginning of migration, during migration and/or towards the end of migration (Gleeson and Walsh, 2000). Of these, classical lissencephaly, also referred to as the agyria-pachygyria spectrum, is caused by a defect during migration that leads to abnormal lamination and a thickened cortex that is characterized by a more-or-less four-layered cortex. Cobblestone lissencephalies are disorders of migration caused by a defect in the integrity of the pial membrane that leads to the formation of breaches during rapid cortical expansion with a disorganization of radial glia end feet and fibres. This results in a massive overmigration of neuroglial cells in the leptomeningeal spaces surrounding the cerebral cortex and in the cerebellum (Moore *et al.*, 2002; Montanaro and Carbonetto, 2003). On the other hand, polymicrogyria is aetiologically and histologically heterogeneous and its pathogenesis remains poorly understood. In polymicrogyria, the normal folding of the cerebral cortex is disrupted, resulting in an irregular surface with numerous smaller and irregular folds (gyri) and shallow, partly fused intervening grooves (sulci). Classically, polymicrogyria is thought to be a disorder of late migration or cortical organization, and supposed to reflect a disruption of normal neuronal migration with subsequent disordered cortical organization (Barkovich *et al.*, 2005).

Interestingly, the foetopathological brain features (i.e. neuronal overmigration, rupture of the pial basement membrane and dysplasic rostral cerebellum) reported in this study are consistent with those described in the developing forebrain and rostral cerebellum of the *GPR56*$^{-/-}$ mouse model (Li *et al.*, 2008; Koirala *et al.*, 2009). They are also reminiscent of those reported in recent studies on β-tubulin 2B-related polymicrogyria (Jaglin *et al.*, 2009; Jaglin and Chelly, 2009; Jackson, 2009).

Given these findings, we are tempted to propose that the pathophysiological processes underlying *GPR56*-related BFPP could result from a combined effect of alterations of pial basement membrane integrity, radial glial organization and neuronal overmigration during critical stages of brain development.

At the molecular level, hypotheses based on insights provided by advances in the understanding of the pathogenesis of cobblestone lissencephalies, which are known to be associated with hypoglycosylation and dysfunction of α-dystroglycan (Henry and Campbell, 1998; Hewitt, 2009), should be considered. Indeed, the fact that *GPR56* encodes a G-protein-coupled receptor expressed in radial glia endfeet suggests that loss of function of *GPR56*, or its altered subcellular localization or glycosylation, is likely to have a deleterious effect on the interaction between the pial basement membrane and radial glial endfeet. This results in a disruption of pial membrane basement integrity, radial glia disorganization and subsequently produces abnormalities of cortical organization and folding.

Taken as a whole, the data reported here open new and exciting insights into the pathophysiology of polymicrogyria, and give further evidence of a continuum of cortical dysgenesis from unlayered polymicrogyria at the less severe end of the spectrum to the cobblestone lissencephalies. They suggest that alterations of the regulation of pial basement membrane integrity during development and overmigration of neuronal cells, characteristics reminiscent of cobblestone lissencephaly (Li *et al.*, 2008), should be taken into consideration when attempting to define the pathophysiological mechanisms underlying polymicrogyria.

Acknowledgements

The authors wish to thank Dr Olivier Dulac for his helpful discussions. We would like to thank the patients and their families, as well as their referring physicians and genetic counsellors (Drs M. Bourgeois and D. Heron), without whom this study would not have been possible. We would like to thank Nathalie Carion for her help in performing molecular analysis. The authors are grateful to Dr A. Kaminska and V. Bouilleret for their help in the analysis of EEG. N.B.B., N.S., E.B., O.C., M.B., I.A., P.D., V.d.P., M.E.M., and M.L.M. recruited human subjects and carried out their phenotype assessment. C.F.B. examined the

foetopathological case. K.P., J.R., L.V. and C.B. performed genetic and molecular investigations. N.B.B. and N.B. re-examined the patient's MRIs. C.E. performed statistical analysis. N.B.B. and C.S. re-examined patients' EEG data. N.B.B. drafted the article with the help of K.P., K.L. and J.C. J.C. supervised the design and follow-up of the study and preparation of the article. N.B.B. and K.P. contributed to the writing of the article. The article was finalized by N.B.B., K.P. and J.C. with the assistance of all co-authors.

Funding

INSERM, CNRS, FRM (Program Equipe FRM-2007) and ANR (ANR-05-Neuro-040-01, ANR MNPS 2008).

References

Aihara M, Tanabe Y, Kato K. Serial MRI in Fukuyama type congenital muscular dystrophy. Neuroradiology 1992; 34: 396–8.

Barkovich AJ. Neuroimaging manifestations and classification of congenital muscular dystrophies. AJNR Am J Neuroradiol 1998; 19: 1389–96.

Barkovich AJ. Congenital malformations of the brain and skull. In: Wilkins LW, editor. Pediatric neuroimaging. Philadelphia: Lippincott Williams & Wilkins; 2005. p. 341–52.

Barkovich AJ, Kuzniecky RI, Jackson GD, Guerrini R, Dobyns WB. A developmental and genetic classification for malformations of cortical development. Neurology 2005; 65: 1873–87.

Beltran-Valero de Bernabe D, Currier S, Steinbrecher A, Celli J, van Beusekom E, van der Zwaag B, et al. Mutations in the O-mannosyltransferase gene POMT1 give rise to the severe neuronal migration disorder Walker-Warburg syndrome. Am J Hum Genet 2002; 71: 1033–43.

Brockington M, Torelli S, Prandini P, Boito C, Dolatshad NF, Longman C, et al. Localization and functional analysis of the LARGE family of glycosyltransferases: significance for muscular dystrophy. Hum Mol Genet 2005; 14: 657–65.

Chang BS, Piao X, Bodell A, Basel-Vanagaite L, Straussberg R, Dobyns WB, et al. Bilateral frontoparietal polymicrogyria: clinical and radiological features in 10 families with linkage to chromosome 16. Ann Neurol 2003; 53: 596–606.

de Rijk-van Andel JF, Arts WF, de Weerd AW. EEG in type I lissencephaly. Dev Med Child Neurol 1988; 30: 126–7.

Della Bernardina B, Perez-Jimenez A, Fontana E, Colamaria V, Piardi F, Avesani E, et al. Electroencephalographic findings associated with cortical dysplasias. In: Guerrini R, editor. Dysplasias of cerebral cortex and epilepsy. Philadelphia: Lippincott-Raven; 1996. p. 235–45.

Dobyns WB, Pagon RA, Armstrong D, Curry CJ, Greenberg F, Grix A, et al. Diagnostic criteria for Walker-Warburg syndrome. Am J Med Genet 1989; 32: 195–210.

Fukuyama Y, Osawa M, Suzuki H. Congenital progressive muscular dystrophy of the Fukuyama type: clinical, genetic and pathological considerations. Brain Dev 1981; 3: 1–29.

Gastaut H, Pinsard N, Raybaud C, Aicardi J, Zifkin B. Lissencephaly (agyria-pachygyria): clinical findings and serial EEG studies. Dev Med Child Neurol 1987; 29: 167–80.

Gleeson JG, Walsh CA. Neuronal migration disorders: from genetic diseases to developmental mechanisms. Trends Neurosci 2000; 23: 352–9.

Godfrey C, Clement E, Mein R, Brockington M, Smith J, Talim B, et al. Refining genotype phenotype correlations in muscular dystrophies with defective glycosylation of dystroglycan. Brain 2007; 130: 2725–35.

Harbord MG, Boyd S, Hall-Craggs MA, Kendall B, McShane MA, Baraitser M. Ataxia, developmental delay and an extensive neuronal migration abnormality in 2 siblings. Neuropediatrics 1990; 21: 218–21.

Henry MD, Campbell KP. A role for dystroglycan in basement membrane assembly. Cell 1998; 95: 859–70.

Hewitt JE. Abnormal glycosylation of dystroglycan in human genetic disease. Biochim Biophys Acta 2009; 1792: 853–61.

Jackson AP. Diversifying microtubules in brain development. Nat Genet 2009; 41: 638–40.

Jaglin XH, Chelly J. Tubulin-related cortical dysgeneses: microtubule dysfunction underlying neuronal migration defects. Trends Genet 2009; 25: 555–66.

Jansen A, Andermann E. Genetics of the polymicrogyria syndromes. J Med Genet 2005; 42: 369–78.

Jin Z, Tietjen I, Bu L, Liu-Yesucevitz L, Gaur SK, Walsh CA, et al. Disease-associated mutations affect GPR56 protein trafficking and cell surface expression. Hum Mol Genet 2007; 16: 1972–85.

Jissendi-Tchofo P, Kara S, Barkovich AJ. Midbrain-hindbrain involvement in lissencephalies. Neurology 2009; 72: 410–8.

Ke N, Sundaram R, Liu G, Chionis J, Fan W, Rogers C, et al. Orphan G protein-coupled receptor GPR56 plays a role in cell transformation and tumorigenesis involving the cell adhesion pathway. Mol Cancer Ther 2007; 6: 1840–50.

Koirala S, Jin Z, Piao X, Corfas G. GPR56-regulated granule cell adhesion is essential for rostral cerebellar development. J Neurosci 2009; 29: 7439–49.

Li S, Jin Z, Koirala S, Bu L, Xu L, Hynes RO, et al. GPR56 regulates pial basement membrane integrity and cortical lamination. J Neurosci 2008; 28: 5817–26.

Mercuri E, Messina S, Bruno C, Mora M, Pegoraro E, Comi GP, et al. Congenital muscular dystrophies with defective glycosylation of dystroglycan: a population study. Neurology 2009; 72: 1802–9.

Mercuri E, Topaloglu H, Brockington M, Berardinelli A, Pichiecchio A, Santorelli F, et al. Spectrum of brain changes in patients with congenital muscular dystrophy and FKRP gene mutations. Arch Neurol 2006; 63: 251–7.

Montanaro F, Carbonetto S. Targeting dystroglycan in the brain. Neuron 2003; 37: 193–6.

Moore SA, Saito F, Chen J, Michele DE, Henry MD, Messing A, et al. Deletion of brain dystroglycan recapitulates aspects of congenital muscular dystrophy. Nature 2002; 418: 422–5.

Mori K, Hashimoto T, Tayama M, Miyazaki M, Fukuda K, Endo S, et al. Serial EEG and sleep polygraphic studies on lissencephaly (agyria-pachygyria). Brain Dev 1994; 16: 365–73.

Parrini E, Ferrari AR, Dorn T, Walsh CA, Guerrini R. Bilateral frontoparietal polymicrogyria, Lennox-Gastaut syndrome, and GPR56 gene mutations. Epilepsia 2009; 50: 1344–53.

Piao X, Basel-Vanagaite L, Straussberg R, Grant PE, Pugh EW, Doheny K, et al. An autosomal recessive form of bilateral frontoparietal polymicrogyria maps to chromosome 16q12.2-21. Am J Hum Genet 2002; 70: 1028–33.

Piao X, Chang BS, Bodell A, Woods K, Benzeev B, Topcu M, et al. Genotype-phenotype analysis of human frontoparietal polymicrogyria syndromes. Ann Neurol 2005; 58: 680–7.

Piao X, Hill RS, Bodell A, Chang BS, Basel-Vanagaite L, Straussberg R, et al. G protein-coupled receptor-dependent development of human frontal cortex. Science 2004; 303: 2033–6.

Raymond AA, Fish DR, Boyd SG, Smith SJ, Pitt MC, Kendall B. Cortical dysgenesis: serial EEG findings in children and adults. Electroencephalogr Clin Neurophysiol 1995; 94: 389–97.

Santanelli P. EEG fast activities in lissencephaly. Ital J Neurol Sci 1991; 12: 122.

Valanne L, Pihko H, Katevuo K, Karttunen P, Somer H, Santavuori P. MRI of the brain in muscle-eye-brain (MEB) disease. Neuroradiology 1994; 36: 473–6.

van der Knaap MS, Smit LM, Barth PG, Catsman-Berrevoets CE, Brouwer OF, Begeer JH, et al. Magnetic resonance imaging in classification of congenital muscular dystrophies with brain abnormalities. Ann Neurol 1997; 42: 50–9.

van Reeuwijk J, Janssen M, van den Elzen C, Beltran-Valero de Bernabe D, Sabatelli P, Merlini L, et al. POMT2 mutations cause α-dystroglycan hypoglycosylation and Walker-Warburg syndrome. J Med Genet 2005; 42: 907–12.